

Evidence for the Decay $B^\pm \rightarrow K^{*\pm}\pi^0$

B. Aubert,¹ R. Barate,¹ D. Boutigny,¹ F. Couderc,¹ Y. Karyotakis,¹ J. P. Lees,¹ V. Poireau,¹ V. Tisserand,¹
A. Zghiche,¹ E. Grauges,² A. Palano,³ M. Pappagallo,³ A. Pompili,³ J. C. Chen,⁴ N. D. Qi,⁴ G. Rong,⁴ P. Wang,⁴
Y. S. Zhu,⁴ G. Eigen,⁵ I. Ofte,⁵ B. Stugu,⁵ G. S. Abrams,⁶ A. W. Borgland,⁶ A. B. Breon,⁶ D. N. Brown,⁶
J. Button-Shafer,⁶ R. N. Cahn,⁶ E. Charles,⁶ C. T. Day,⁶ M. S. Gill,⁶ A. V. Gritsan,⁶ Y. Groysman,⁶
R. G. Jacobsen,⁶ R. W. Kadel,⁶ J. Kadyk,⁶ L. T. Kerth,⁶ Yu. G. Kolomensky,⁶ G. Kukartsev,⁶ G. Lynch,⁶
L. M. Mir,⁶ P. J. Oddone,⁶ T. J. Orimoto,⁶ M. Pripstein,⁶ N. A. Roe,⁶ M. T. Ronan,⁶ W. A. Wenzel,⁶ M. Barrett,⁷
K. E. Ford,⁷ T. J. Harrison,⁷ A. J. Hart,⁷ C. M. Hawkes,⁷ S. E. Morgan,⁷ A. T. Watson,⁷ M. Fritsch,⁸ K. Goetzen,⁸
T. Held,⁸ H. Koch,⁸ B. Lewandowski,⁸ M. Pelizaeus,⁸ K. Peters,⁸ T. Schroeder,⁸ M. Steinke,⁸ J. T. Boyd,⁹
J. P. Burke,⁹ N. Chevalier,⁹ W. N. Cottingham,⁹ M. P. Kelly,⁹ T. Cuhadar-Donszelmann,¹⁰ C. Hearty,¹⁰
N. S. Knecht,¹⁰ T. S. Mattison,¹⁰ J. A. McKenna,¹⁰ D. Thiessen,¹⁰ A. Khan,¹¹ P. Kyberd,¹¹ L. Teodorescu,¹¹
A. E. Blinov,¹² V. E. Blinov,¹² A. D. Bukin,¹² V. P. Druzhinin,¹² V. B. Golubev,¹² V. N. Ivanchenko,¹²
E. A. Kravchenko,¹² A. P. Onuchin,¹² S. I. Serebnyakov,¹² Yu. I. Skovpen,¹² E. P. Solodov,¹² A. N. Yushkov,¹²
D. Best,¹³ M. Bondioli,¹³ M. Bruinsma,¹³ M. Chao,¹³ I. Eschrich,¹³ D. Kirkby,¹³ A. J. Lankford,¹³ M. Mandelkern,¹³
R. K. Mommsen,¹³ W. Roethel,¹³ D. P. Stoker,¹³ C. Buchanan,¹⁴ B. L. Hartfiel,¹⁴ A. J. R. Weinstein,¹⁴
S. D. Foulkes,¹⁵ J. W. Gary,¹⁵ O. Long,¹⁵ B. C. Shen,¹⁵ K. Wang,¹⁵ L. Zhang,¹⁵ D. del Re,¹⁶ H. K. Hadavand,¹⁶
E. J. Hill,¹⁶ D. B. MacFarlane,¹⁶ H. P. Paar,¹⁶ S. Rahatlou,¹⁶ V. Sharma,¹⁶ J. W. Berryhill,¹⁷ C. Campagnari,¹⁷
A. Cunha,¹⁷ B. Dahmes,¹⁷ T. M. Hong,¹⁷ A. Lu,¹⁷ M. A. Mazur,¹⁷ J. D. Richman,¹⁷ W. Verkerke,¹⁷ T. W. Beck,¹⁸
A. M. Eisner,¹⁸ C. J. Flacco,¹⁸ C. A. Heusch,¹⁸ J. Kroseberg,¹⁸ W. S. Lockman,¹⁸ G. Nesom,¹⁸ T. Schalk,¹⁸
B. A. Schumm,¹⁸ A. Seiden,¹⁸ P. Spradlin,¹⁸ D. C. Williams,¹⁸ M. G. Wilson,¹⁸ J. Albert,¹⁹ E. Chen,¹⁹
G. P. Dubois-Felsmann,¹⁹ A. Dvoretzki,¹⁹ D. G. Hitlin,¹⁹ I. Narsky,¹⁹ T. Piatenko,¹⁹ F. C. Porter,¹⁹ A. Ryd,¹⁹
A. Samuel,¹⁹ S. Yang,¹⁹ R. Andreassen,²⁰ S. Jayatilake,²⁰ G. Mancinelli,²⁰ B. T. Meadows,²⁰ M. D. Sokoloff,²⁰
F. Blanc,²¹ P. Bloom,²¹ S. Chen,²¹ W. T. Ford,²¹ U. Nauenberg,²¹ A. Olivas,²¹ P. Rankin,²¹ W. O. Ruddick,²¹
J. G. Smith,²¹ K. A. Ulmer,²¹ J. Zhang,²¹ A. Chen,²² E. A. Eckhart,²² J. L. Harton,²² A. Soffer,²² W. H. Toki,²²
R. J. Wilson,²² Q. Zeng,²² B. Spaan,²³ D. Altenburg,²⁴ T. Brandt,²⁴ J. Brose,²⁴ M. Dickopp,²⁴ E. Feltresi,²⁴
A. Hauke,²⁴ V. Klose,²⁴ H. M. Lacker,²⁴ E. Maly,²⁴ R. Nogowski,²⁴ S. Otto,²⁴ A. Petzold,²⁴ G. Schott,²⁴
J. Schubert,²⁴ K. R. Schubert,²⁴ R. Schwierz,²⁴ J. E. Sundermann,²⁴ D. Bernard,²⁵ G. R. Bonneaud,²⁵ P. Grenier,²⁵
S. Schrenk,²⁵ Ch. Thiebaux,²⁵ G. Vasileiadis,²⁵ M. Verderi,²⁵ D. J. Bard,²⁶ P. J. Clark,²⁶ W. Gradl,²⁶ F. Muheim,²⁶
S. Playfer,²⁶ Y. Xie,²⁶ M. Andreotti,²⁷ V. Azzolini,²⁷ D. Bettoni,²⁷ C. Bozzi,²⁷ R. Calabrese,²⁷ G. Cibinetto,²⁷
E. Luppi,²⁷ M. Negrini,²⁷ L. Piemontese,²⁷ A. Sarti,²⁷ F. Anulli,²⁸ R. Baldini-Ferrolli,²⁸ A. Calcaterra,²⁸ R. de
Sangro,²⁸ G. Finocchiaro,²⁸ P. Patteri,²⁸ I. M. Peruzzi,²⁸ M. Piccolo,²⁸ A. Zallo,²⁸ A. Buzzo,²⁹ R. Capra,²⁹
R. Contri,²⁹ M. Lo Vetere,²⁹ M. Macri,²⁹ M. R. Monge,²⁹ S. Passaggio,²⁹ C. Patrignani,²⁹ E. Robutti,²⁹
A. Santroni,²⁹ S. Tosi,²⁹ S. Bailey,³⁰ G. Brandenburg,³⁰ K. S. Chaisanguanthum,³⁰ M. Morii,³⁰ E. Won,³⁰
R. S. Dubitzky,³¹ U. Langenegger,³¹ J. Marks,³¹ S. Schenk,³¹ U. Uwer,³¹ W. Bhimji,³² D. A. Bowerman,³²
P. D. Dauncey,³² U. Egede,³² J. R. Gaillard,³² G. W. Morton,³² J. A. Nash,³² M. B. Nikolich,³² G. P. Taylor,³²
M. J. Charles,³³ G. J. Grenier,³³ U. Mallik,³³ A. K. Mohapatra,³³ J. Cochran,³⁴ H. B. Crawley,³⁴ V. Eyges,³⁴
W. T. Meyer,³⁴ S. Prell,³⁴ E. I. Rosenberg,³⁴ A. E. Rubin,³⁴ J. Yi,³⁴ N. Arnaud,³⁵ M. Davier,³⁵ X. Giroux,³⁵
G. Grosdidier,³⁵ A. Höcker,³⁵ F. Le Diberder,³⁵ V. Lepeltier,³⁵ A. M. Lutz,³⁵ T. C. Petersen,³⁵ M. Pierini,³⁵
S. Plaszczynski,³⁵ S. Rodier,³⁵ P. Roudeau,³⁵ M. H. Schune,³⁵ A. Stocchi,³⁵ G. Wormser,³⁵ C. H. Cheng,³⁶
D. J. Lange,³⁶ M. C. Simani,³⁶ D. M. Wright,³⁶ A. J. Bevan,³⁷ C. A. Chavez,³⁷ J. P. Coleman,³⁷ I. J. Forster,³⁷
J. R. Fry,³⁷ E. Gabathuler,³⁷ R. Gamet,³⁷ K. A. George,³⁷ D. E. Hutchcroft,³⁷ R. J. Parry,³⁷ D. J. Payne,³⁷
C. Touramanis,³⁷ C. M. Cormack,³⁸ F. Di Lodovico,³⁸ C. L. Brown,³⁹ G. Cowan,³⁹ R. L. Flack,³⁹ H. U. Flaecher,³⁹
M. G. Green,³⁹ P. S. Jackson,³⁹ T. R. McMahon,³⁹ S. Ricciardi,³⁹ F. Salvatore,³⁹ D. Brown,⁴⁰ C. L. Davis,⁴⁰
J. Allison,⁴¹ N. R. Barlow,⁴¹ R. J. Barlow,⁴¹ M. C. Hodgkinson,⁴¹ G. D. Lafferty,⁴¹ M. T. Naisbit,⁴¹
J. C. Williams,⁴¹ C. Chen,⁴² A. Farbin,⁴² W. D. Hulsbergen,⁴² A. Jawahery,⁴² D. Kovalskyi,⁴² C. K. Lae,⁴²
V. Lillard,⁴² D. A. Roberts,⁴² G. Blaylock,⁴³ C. Dallapiccola,⁴³ S. S. Hertzbach,⁴³ R. Kofler,⁴³ V. B. Koptchev,⁴³
T. B. Moore,⁴³ S. Saremi,⁴³ H. Staengle,⁴³ S. Willocq,⁴³ R. Cowan,⁴⁴ K. Koeneke,⁴⁴ G. Sciolla,⁴⁴ S. J. Sekula,⁴⁴
F. Taylor,⁴⁴ R. K. Yamamoto,⁴⁴ H. Kim,⁴⁵ P. M. Patel,⁴⁵ S. H. Robertson,⁴⁵ A. Lazzaro,⁴⁶ V. Lombardo,⁴⁶
F. Palombo,⁴⁶ J. M. Bauer,⁴⁷ L. Cremaldi,⁴⁷ V. Eschenburg,⁴⁷ R. Godang,⁴⁷ R. Kroeger,⁴⁷ J. Reidy,⁴⁷
D. A. Sanders,⁴⁷ D. J. Summers,⁴⁷ H. W. Zhao,⁴⁷ S. Brunet,⁴⁸ D. Côté,⁴⁸ P. Taras,⁴⁸ B. Viaud,⁴⁸ H. Nicholson,⁴⁹
N. Cavallo,⁵⁰ * G. De Nardo,⁵⁰ F. Fabozzi,⁵⁰ * C. Gatto,⁵⁰ L. Lista,⁵⁰ D. Monorchio,⁵⁰ P. Paolucci,⁵⁰ D. Piccolo,⁵⁰
C. Sciacca,⁵⁰ M. Baak,⁵¹ H. Bulten,⁵¹ G. Raven,⁵¹ H. L. Snoek,⁵¹ L. Wilden,⁵¹ C. P. Jessop,⁵² J. M. LoSecco,⁵²
T. Allmendinger,⁵³ G. Benelli,⁵³ K. K. Gan,⁵³ K. Honscheid,⁵³ D. Hufnagel,⁵³ P. D. Jackson,⁵³ H. Kagan,⁵³

R. Kass,⁵³ T. Pulliam,⁵³ A. M. Rahimi,⁵³ R. Ter-Antonyan,⁵³ Q. K. Wong,⁵³ J. Brau,⁵⁴ R. Frey,⁵⁴ O. Igonkina,⁵⁴ M. Lu,⁵⁴ C. T. Potter,⁵⁴ N. B. Sinev,⁵⁴ D. Strom,⁵⁴ E. Torrence,⁵⁴ F. Colecchia,⁵⁵ A. Dorigo,⁵⁵ F. Galeazzi,⁵⁵ M. Margoni,⁵⁵ M. Morandin,⁵⁵ M. Posocco,⁵⁵ M. Rotondo,⁵⁵ F. Simonetto,⁵⁵ R. Stroili,⁵⁵ C. Voci,⁵⁵ M. Benayoun,⁵⁶ H. Briand,⁵⁶ J. Chauveau,⁵⁶ P. David,⁵⁶ L. Del Buono,⁵⁶ Ch. de la Vaissière,⁵⁶ O. Hamon,⁵⁶ M. J. J. John,⁵⁶ Ph. Leruste,⁵⁶ J. Malclès,⁵⁶ J. Ocariz,⁵⁶ L. Roos,⁵⁶ G. Therin,⁵⁶ P. K. Behera,⁵⁷ L. Gladney,⁵⁷ Q. H. Guo,⁵⁷ J. Panetta,⁵⁷ M. Biasini,⁵⁸ R. Covarelli,⁵⁸ M. Pioppi,⁵⁸ C. Angelini,⁵⁹ G. Batignani,⁵⁹ S. Bettarini,⁵⁹ F. Bucci,⁵⁹ G. Calderini,⁵⁹ M. Carpinelli,⁵⁹ F. Forti,⁵⁹ M. A. Giorgi,⁵⁹ A. Lusiani,⁵⁹ G. Marchiori,⁵⁹ M. Morganti,⁵⁹ N. Neri,⁵⁹ E. Paoloni,⁵⁹ M. Rama,⁵⁹ G. Rizzo,⁵⁹ G. Simi,⁵⁹ J. Walsh,⁵⁹ M. Haire,⁶⁰ D. Judd,⁶⁰ K. Paick,⁶⁰ D. E. Wagoner,⁶⁰ J. Biesiada,⁶¹ N. Danielson,⁶¹ P. Elmer,⁶¹ Y. P. Lau,⁶¹ C. Lu,⁶¹ J. Olsen,⁶¹ A. J. S. Smith,⁶¹ A. V. Telnov,⁶¹ F. Bellini,⁶² G. Cavoto,⁶² A. D’Orazio,⁶² E. Di Marco,⁶² R. Faccini,⁶² F. Ferrarotto,⁶² F. Ferroni,⁶² M. Gaspero,⁶² L. Li Gioi,⁶² M. A. Mazzoni,⁶² S. Morganti,⁶² G. Piredda,⁶² F. Polci,⁶² F. Safai Tehrani,⁶² C. Voena,⁶² S. Christ,⁶³ H. Schröder,⁶³ G. Wagner,⁶³ R. Waldi,⁶³ T. Adye,⁶⁴ N. De Groot,⁶⁴ B. Franek,⁶⁴ G. P. Gopal,⁶⁴ E. O. Olaiya,⁶⁴ F. F. Wilson,⁶⁴ R. Aleksan,⁶⁵ S. Emery,⁶⁵ A. Gaidot,⁶⁵ S. F. Ganzhur,⁶⁵ P.-F. Giraud,⁶⁵ G. Graziani,⁶⁵ G. Hamel de Monchenault,⁶⁵ W. Kozanecki,⁶⁵ M. Legendre,⁶⁵ G. W. London,⁶⁵ B. Mayer,⁶⁵ G. Vasseur,⁶⁵ Ch. Yèche,⁶⁵ M. Zito,⁶⁵ M. V. Purohit,⁶⁶ A. W. Weidemann,⁶⁶ J. R. Wilson,⁶⁶ F. X. Yumiceva,⁶⁶ T. Abe,⁶⁷ M. T. Allen,⁶⁷ D. Aston,⁶⁷ R. Bartoldus,⁶⁷ N. Berger,⁶⁷ A. M. Boyarski,⁶⁷ O. L. Buchmueller,⁶⁷ R. Claus,⁶⁷ M. R. Convery,⁶⁷ M. Cristinziani,⁶⁷ J. C. Dingfelder,⁶⁷ D. Dong,⁶⁷ J. Dorfan,⁶⁷ D. Dujmic,⁶⁷ W. Dunwoodie,⁶⁷ S. Fan,⁶⁷ R. C. Field,⁶⁷ T. Glanzman,⁶⁷ S. J. Gowdy,⁶⁷ T. Hadig,⁶⁷ V. Halyo,⁶⁷ C. Hast,⁶⁷ T. Hryn’ova,⁶⁷ W. R. Innes,⁶⁷ S. Kazuhito,⁶⁷ M. H. Kelsey,⁶⁷ P. Kim,⁶⁷ M. L. Kocian,⁶⁷ D. W. G. S. Leith,⁶⁷ J. Libby,⁶⁷ S. Luitz,⁶⁷ V. Luth,⁶⁷ H. L. Lynch,⁶⁷ H. Marsiske,⁶⁷ R. Messner,⁶⁷ D. R. Muller,⁶⁷ C. P. O’Grady,⁶⁷ V. E. Ozcan,⁶⁷ A. Perazzo,⁶⁷ M. Perl,⁶⁷ B. N. Ratcliff,⁶⁷ A. Roodman,⁶⁷ A. A. Salnikov,⁶⁷ R. H. Schindler,⁶⁷ J. Schwiening,⁶⁷ A. Snyder,⁶⁷ A. Soha,⁶⁷ J. Stelzer,⁶⁷ J. Strube,^{54, 67} D. Su,⁶⁷ M. K. Sullivan,⁶⁷ J. M. Thompson,⁶⁷ J. Va’vra,⁶⁷ S. R. Wagner,⁶⁷ M. Weaver,⁶⁷ W. J. Wisniewski,⁶⁷ M. Wittgen,⁶⁷ D. H. Wright,⁶⁷ A. K. Yarritu,⁶⁷ C. C. Young,⁶⁷ P. R. Burchat,⁶⁸ A. J. Edwards,⁶⁸ S. A. Majewski,⁶⁸ B. A. Petersen,⁶⁸ C. Roat,⁶⁸ M. Ahmed,⁶⁹ S. Ahmed,⁶⁹ M. S. Alam,⁶⁹ J. A. Ernst,⁶⁹ M. A. Saeed,⁶⁹ M. Saleem,⁶⁹ F. R. Wappler,⁶⁹ W. Bugg,⁷⁰ M. Krishnamurthy,⁷⁰ S. M. Spanier,⁷⁰ R. Eckmann,⁷¹ J. L. Ritchie,⁷¹ A. Satpathy,⁷¹ R. F. Schwitters,⁷¹ J. M. Izen,⁷² I. Kitayama,⁷² X. C. Lou,⁷² S. Ye,⁷² F. Bianchi,⁷³ M. Bona,⁷³ F. Gallo,⁷³ D. Gamba,⁷³ M. Bomben,⁷⁴ L. Bosisio,⁷⁴ C. Cartaro,⁷⁴ F. Cossutti,⁷⁴ G. Della Ricca,⁷⁴ S. Dittongo,⁷⁴ S. Grancagnolo,⁷⁴ L. Lanceri,⁷⁴ P. Poropat,⁷⁴ † L. Vitale,⁷⁴ G. Vuagnin,⁷⁴ F. Martinez-Vidal,⁷⁵ R. S. Panvini,⁷⁶ † Sw. Banerjee,⁷⁷ B. Bhuyan,⁷⁷ C. M. Brown,⁷⁷ D. Fortin,⁷⁷ K. Hamano,⁷⁷ R. Kowalewski,⁷⁷ J. M. Roney,⁷⁷ R. J. Sobie,⁷⁷ J. J. Back,⁷⁸ P. F. Harrison,⁷⁸ T. E. Latham,⁷⁸ G. B. Mohanty,⁷⁸ H. R. Band,⁷⁹ X. Chen,⁷⁹ B. Cheng,⁷⁹ S. Dasu,⁷⁹ M. Datta,⁷⁹ A. M. Eichenbaum,⁷⁹ K. T. Flood,⁷⁹ M. Graham,⁷⁹ J. J. Hollar,⁷⁹ J. R. Johnson,⁷⁹ P. E. Kutter,⁷⁹ H. Li,⁷⁹ R. Liu,⁷⁹ B. Mellado,⁷⁹ A. Mihalyi,⁷⁹ Y. Pan,⁷⁹ R. Prepost,⁷⁹ P. Tan,⁷⁹ J. H. von Wimmersperg-Toeller,⁷⁹ J. Wu,⁷⁹ S. L. Wu,⁷⁹ Z. Yu,⁷⁹ M. G. Greene,⁸⁰ and H. Neal⁸⁰

(The BABAR Collaboration)

¹Laboratoire de Physique des Particules, F-74941 Annecy-le-Vieux, France

²IFAE, Universitat Autònoma de Barcelona, E-08193 Bellaterra, Barcelona, Spain

³Università di Bari, Dipartimento di Fisica and INFN, I-70126 Bari, Italy

⁴Institute of High Energy Physics, Beijing 100039, China

⁵University of Bergen, Inst. of Physics, N-5007 Bergen, Norway

⁶Lawrence Berkeley National Laboratory and University of California, Berkeley, California 94720, USA

⁷University of Birmingham, Birmingham, B15 2TT, United Kingdom

⁸Ruhr Universität Bochum, Institut für Experimentalphysik 1, D-44780 Bochum, Germany

⁹University of Bristol, Bristol BS8 1TL, United Kingdom

¹⁰University of British Columbia, Vancouver, British Columbia, Canada V6T 1Z1

¹¹Brunel University, Uxbridge, Middlesex UB8 3PH, United Kingdom

¹²Budker Institute of Nuclear Physics, Novosibirsk 630090, Russia

¹³University of California at Irvine, Irvine, California 92697, USA

¹⁴University of California at Los Angeles, Los Angeles, California 90024, USA

¹⁵University of California at Riverside, Riverside, California 92521, USA

¹⁶University of California at San Diego, La Jolla, California 92093, USA

¹⁷University of California at Santa Barbara, Santa Barbara, California 93106, USA

¹⁸University of California at Santa Cruz, Institute for Particle Physics, Santa Cruz, California 95064, USA

¹⁹California Institute of Technology, Pasadena, California 91125, USA

²⁰University of Cincinnati, Cincinnati, Ohio 45221, USA

²¹University of Colorado, Boulder, Colorado 80309, USA

²²Colorado State University, Fort Collins, Colorado 80523, USA

- ²³Universität Dortmund, Institut für Physik, D-44221 Dortmund, Germany
- ²⁴Technische Universität Dresden, Institut für Kern- und Teilchenphysik, D-01062 Dresden, Germany
- ²⁵Ecole Polytechnique, LLR, F-91128 Palaiseau, France
- ²⁶University of Edinburgh, Edinburgh EH9 3JZ, United Kingdom
- ²⁷Università di Ferrara, Dipartimento di Fisica and INFN, I-44100 Ferrara, Italy
- ²⁸Laboratori Nazionali di Frascati dell'INFN, I-00044 Frascati, Italy
- ²⁹Università di Genova, Dipartimento di Fisica and INFN, I-16146 Genova, Italy
- ³⁰Harvard University, Cambridge, Massachusetts 02138, USA
- ³¹Universität Heidelberg, Physikalisches Institut, Philosophenweg 12, D-69120 Heidelberg, Germany
- ³²Imperial College London, London, SW7 2AZ, United Kingdom
- ³³University of Iowa, Iowa City, Iowa 52242, USA
- ³⁴Iowa State University, Ames, Iowa 50011-3160, USA
- ³⁵Laboratoire de l'Accélérateur Linéaire, F-91898 Orsay, France
- ³⁶Lawrence Livermore National Laboratory, Livermore, California 94550, USA
- ³⁷University of Liverpool, Liverpool L69 7ZE, United Kingdom
- ³⁸Queen Mary, University of London, E1 4NS, United Kingdom
- ³⁹University of London, Royal Holloway and Bedford New College, Egham, Surrey TW20 0EX, United Kingdom
- ⁴⁰University of Louisville, Louisville, Kentucky 40292, USA
- ⁴¹University of Manchester, Manchester M13 9PL, United Kingdom
- ⁴²University of Maryland, College Park, Maryland 20742, USA
- ⁴³University of Massachusetts, Amherst, Massachusetts 01003, USA
- ⁴⁴Massachusetts Institute of Technology, Laboratory for Nuclear Science, Cambridge, Massachusetts 02139, USA
- ⁴⁵McGill University, Montréal, Quebec, Canada H3A 2T8
- ⁴⁶Università di Milano, Dipartimento di Fisica and INFN, I-20133 Milano, Italy
- ⁴⁷University of Mississippi, University, Mississippi 38677, USA
- ⁴⁸Université de Montréal, Laboratoire René J. A. Lévesque, Montréal, Quebec, Canada H3C 3J7
- ⁴⁹Mount Holyoke College, South Hadley, Massachusetts 01075, USA
- ⁵⁰Università di Napoli Federico II, Dipartimento di Scienze Fisiche and INFN, I-80126, Napoli, Italy
- ⁵¹NIKHEF, National Institute for Nuclear Physics and High Energy Physics, NL-1009 DB Amsterdam, The Netherlands
- ⁵²University of Notre Dame, Notre Dame, Indiana 46556, USA
- ⁵³Ohio State University, Columbus, Ohio 43210, USA
- ⁵⁴University of Oregon, Eugene, Oregon 97403, USA
- ⁵⁵Università di Padova, Dipartimento di Fisica and INFN, I-35131 Padova, Italy
- ⁵⁶Universités Paris VI et VII, Laboratoire de Physique Nucléaire et de Hautes Energies, F-75252 Paris, France
- ⁵⁷University of Pennsylvania, Philadelphia, Pennsylvania 19104, USA
- ⁵⁸Università di Perugia, Dipartimento di Fisica and INFN, I-06100 Perugia, Italy
- ⁵⁹Università di Pisa, Dipartimento di Fisica, Scuola Normale Superiore and INFN, I-56127 Pisa, Italy
- ⁶⁰Prairie View A&M University, Prairie View, Texas 77446, USA
- ⁶¹Princeton University, Princeton, New Jersey 08544, USA
- ⁶²Università di Roma La Sapienza, Dipartimento di Fisica and INFN, I-00185 Roma, Italy
- ⁶³Universität Rostock, D-18051 Rostock, Germany
- ⁶⁴Rutherford Appleton Laboratory, Chilton, Didcot, Oxon, OX11 0QX, United Kingdom
- ⁶⁵DSM/Dapnia, CEA/Saclay, F-91191 Gif-sur-Yvette, France
- ⁶⁶University of South Carolina, Columbia, South Carolina 29208, USA
- ⁶⁷Stanford Linear Accelerator Center, Stanford, California 94309, USA
- ⁶⁸Stanford University, Stanford, California 94305-4060, USA
- ⁶⁹State University of New York, Albany, New York 12222, USA
- ⁷⁰University of Tennessee, Knoxville, Tennessee 37996, USA
- ⁷¹University of Texas at Austin, Austin, Texas 78712, USA
- ⁷²University of Texas at Dallas, Richardson, Texas 75083, USA
- ⁷³Università di Torino, Dipartimento di Fisica Sperimentale and INFN, I-10125 Torino, Italy
- ⁷⁴Università di Trieste, Dipartimento di Fisica and INFN, I-34127 Trieste, Italy
- ⁷⁵IFIC, Universitat de Valencia-CSIC, E-46071 Valencia, Spain
- ⁷⁶Vanderbilt University, Nashville, Tennessee 37235, USA
- ⁷⁷University of Victoria, Victoria, British Columbia, Canada V8W 3P6
- ⁷⁸Department of Physics, University of Warwick, Coventry CV4 7AL, United Kingdom
- ⁷⁹University of Wisconsin, Madison, Wisconsin 53706, USA
- ⁸⁰Yale University, New Haven, Connecticut 06511, USA

(Dated: April 6, 2005)

We have measured the process $B^\pm \rightarrow (K^{*\pm} \rightarrow K^\pm \pi^0) \pi^0$ with 232 million $\Upsilon(4S) \rightarrow B\bar{B}$ decays collected with the BABAR detector at the PEP-II asymmetric-energy B Factory at SLAC. From a signal yield of 89 ± 26 events we obtain the branching fraction $\mathcal{B}(B^\pm \rightarrow K^{*\pm} \pi^0) = [6.9 \pm 2.0(stat) \pm$

$1.3(\text{sys})] \times 10^{-6}$ with a statistical significance of 3.6 standard deviations including systematic uncertainties, and a charge asymmetry of $0.04 \pm 0.29(\text{stat}) \pm 0.05(\text{sys})$.

PACS numbers: 11.30.Er, 13.25.Hw

Branching fraction and CP -asymmetry measurements of charmless B -meson decays provide valuable constraints for the determination of the unitarity triangle constructed from elements of the Cabibbo-Kobayashi-Maskawa quark-mixing matrix [1, 2]. They test the accuracy of theoretical models such as those based on QCD factorization [3] or SU(3) flavor symmetry [4]. It has been argued that the influence of final-state interactions like charming penguins [5, 6, 7] and similar long-distance rescattering effects [8] on both the branching fraction and CP asymmetry of $B \rightarrow K\pi$ decays may be significant. In this context, the decay $B^\pm \rightarrow K^{*\pm}\pi^0$ is particularly interesting in the light of recent measurements of direct CP -violation in the $B^0 \rightarrow K^\pm\pi^\mp$ and $B^\pm \rightarrow K^\pm\pi^0$ channels [9, 10, 11]. Comparison to the $B^\pm \rightarrow K^{*0}\pi^\pm$ decay mode [12] can provide information about the dominance of penguin diagrams. Here we present a measurement of the branching fraction $\mathcal{B}(B^\pm \rightarrow K^*(892)^\pm\pi^0)$ and its charge asymmetry

$$\mathcal{A}_{CP} = \frac{N(B^- \rightarrow K^{*-}\pi^0) - N(B^+ \rightarrow K^{*+}\pi^0)}{N(B^- \rightarrow K^{*-}\pi^0) + N(B^+ \rightarrow K^{*+}\pi^0)}$$

based exclusively on B^\pm decays to the $K^\pm\pi^0\pi^0$ final state. The data used in this analysis were collected with the BABAR detector [13] at the PEP-II asymmetric-energy e^+e^- storage ring at SLAC. Charged-particle trajectories are measured by a five-layer double-sided silicon vertex tracker and a 40-layer drift chamber located within a 1.5-T solenoidal magnetic field. Charged hadrons are identified by combining energy-loss information from tracking with the measurements from a ring-imaging Cherenkov detector. Photons are detected by a CsI(Tl) crystal electromagnetic calorimeter with an energy resolution of $\sigma_E/E = 0.023(E/\text{GeV})^{-1/4} \oplus 0.014$. The magnet's flux return is instrumented for muon and K_L^0 identification.

The data sample includes 232 ± 3 million $B\bar{B}$ pairs collected at the $\Upsilon(4S)$ resonance, corresponding to an integrated luminosity of 211 fb^{-1} . It is assumed that neutral and charged B meson pairs are produced in equal numbers [14]. In addition, 22 fb^{-1} of data collected at 40 MeV below the $\Upsilon(4S)$ resonance mass were used for background studies. We performed full detector Monte Carlo (MC) simulations equivalent to 460 fb^{-1} of generic $B\bar{B}$ decays and 140 fb^{-1} of continuum quark-antiquark production events. In addition, we simulated over 30 exclusive charmless B decay modes, including 1.2 million signal $B^\pm \rightarrow K^{*\pm}\pi^0$ decays.

B meson candidates are reconstructed from one charged track and two neutral pions. The charged track used to form the $B^\pm \rightarrow K^{*\pm}\pi^0$ candidate is required to have at least 12 hits in the drift chamber, to have a transverse momentum greater than 0.1 GeV/c, and to be consistent with originating from a B -meson decay. Its signal in the tracking and Cherenkov detectors is required to be consistent with that of a kaon. The kaon selection algorithm is 70–92% efficient within the relevant momentum range, with a misidentification rate of less than 7%. We remove tracks that pass electron selection criteria based on dE/dx and calorimeter information. Neutral pion candidates are formed from two photons, each with a minimum energy of 0.03 GeV and a lateral moment [15] of their shower energy deposition greater than zero and less than 0.6. The angular acceptance of photons is restricted to exclude parts of the calorimeter where showers are not fully contained. We require the photon clusters forming the π^0 to be separated in space, with a π^0 energy of at least 0.2 GeV and an invariant mass between 0.10 and 0.16 GeV/c².

Two kinematic variables, $\Delta E = E_B^* - \sqrt{s}/2$ and the beam energy substituted mass $m_{ES} = \sqrt{(s/2 + \mathbf{p}_0 \cdot \mathbf{p}_B)^2/E_0^2 - \mathbf{p}_B^2}$, are used for the final selection of events. Here E_B^* is the B -meson-candidate energy in the center-of-mass frame, E_0 and \sqrt{s} are the total energies of the e^+e^- system in the laboratory and center-of-mass frames, respectively, and \mathbf{p}_0 and \mathbf{p}_B are the three-momenta of the e^+e^- system and the B candidate in the laboratory frame. For correctly reconstructed $K^{*\pm}\pi^0$ candidates ΔE peaks at zero, while final states with a charged pion, such as $B^\pm \rightarrow \rho^\pm\pi^0$, shift ΔE by approximately 80 MeV on average. Events are selected with $5.20 < m_{ES} < 5.29 \text{ GeV}/c^2$ and $|\Delta E| < 0.20 \text{ GeV}$. The ΔE limits help remove background from two- and four-body B decays at a small cost to signal efficiency.

Continuum quark-antiquark production is the dominant background. To suppress it, we select only those events where the angle θ_{Sph}^B in the center-of-mass frame between the direction of the B -meson-candidate and the sphericity axis of the rest of the event satisfies $|\cos\theta_{\text{Sph}}^B| < 0.9$. In addition, we construct a non-linear discriminant, implemented as an artificial neural network (ANN) that uses three input parameters: the zeroth- and second-order Legendre event shape polynomials L_0, L_2 of the momenta and polar angles of all candidates in the rest of the event, and the output of a multivariate, non-linear B -meson-candidate tagging algorithm [16]. ANN is peaked at 0.5 for continuum-like events and at 1.0 for B decays. We require $ANN > 0.58$ for our event selection. To further improve the signal-to-background ratio we restrict the effective invariant mass of the K^* candidate to $0.8 < m_{K\pi} < 1.0 \text{ GeV}/c^2$. Neutral-pion combinatorics

*Also with Università della Basilicata, Potenza, Italy

†Deceased

lead to 30% of our signal events having more than one candidate per event. We choose the best candidate based on a χ^2 formed from the measured masses of the two π^0 candidates within the event compared to the known π^0 mass [17].

After the selection described above, the $B^\pm \rightarrow K^{*\pm}\pi^0$ selection efficiency is 16.5%. In MC studies, the signal candidate is correctly reconstructed (64.5 ± 6.5)% of the time. The remaining candidates come from self-cross-feed (SCF) events, which stem primarily from swapping the low energy π^0 from the resonance with another from the rest of the event. The fraction of SCF events in which the track was swapped with an oppositely charged track was found to be negligible.

MC events are used to study backgrounds from other B -meson decays. The dominant contribution comes from $b \rightarrow c$ transitions; the next most important is from charmless B -meson decays. The latter tend to be more problematic as the branching fractions are often poorly known, and because they may peak at the same invariant mass as the signal $B^\pm \rightarrow K^{*\pm}\pi^0$ events. Thirteen individual charmless modes show a significant contribution once the event selection has been applied. These modes are added into the fit fixed at the yield and asymmetry determined by the simulation. Wherever branching fractions are not available, we use half the upper limit. If no charge asymmetry measurement is available, we assume zero asymmetry.

Although all other known resonant K^* states – subsequently referred to as K^{**} – lie outside our $K^*(892)$ mass window, some may still contribute due to their large width. To estimate the contribution to the signal we select a region in the $K^\pm\pi^0$ invariant mass between 1.2 and 1.6 GeV/ c^2 , motivated by the presence of the broad $K_0^*(1430)$ resonance which decays predominantly to $K\pi$. In this region we make a full maximum likelihood fit to the three variables ΔE , m_{ES} and ANN in an analogous way to how we fit our signal (see below), and extrapolate the result of this fit to the $K^*(892)$ signal region using a $B^\pm \rightarrow K_0^*(1430)^\pm\pi^0$ MC. The fit to the $K_0^*(1430)$ region yields 263 ± 34 events, which translates to 34 K^{**} events contributing to the background in our signal region. We assign a 100% systematic uncertainty to this number to cover possible interference effects as well as uncertainty arising from the lineshapes of K^{**} resonances, which are not well established.

The non-resonant $B^\pm \rightarrow K^\pm\pi^0\pi^0$ branching fraction has, to date, not been measured. To estimate the significance of its contribution we select a region of the Dalitz plot of $m_{K\pi}^2$ – for the π^0 from primary and secondary decay – that is far from the signal as well as $K^*(1430)$ and higher K^{**} resonances and which has low levels of continuum background. A likelihood fit in this region yields 6 ± 8 events, which translates into less than three events in our K^* signal region, assuming the non-resonant events are distributed evenly across the Dalitz plot. We consequently deem the non-resonant contribution negligible.

An unbinned maximum likelihood fit to the variables

m_{ES} , ΔE , $m_{K\pi}$, and ANN is used to extract the total number of signal $B^\pm \rightarrow K^{*\pm}\pi^0$ and continuum background events and their respective charge asymmetries. The likelihood for the selected sample is given by the product of the probability density functions (PDF) for each individual candidate, multiplied by the Poisson factor:

$$\mathcal{L} = \frac{1}{N!} e^{-N'} (N')^N \prod_{i=1}^N \mathcal{P}_i,$$

where N and N' are the number of observed and expected events, respectively. The PDF \mathcal{P}_i for a given event i is the sum of the signal and background terms:

$$\begin{aligned} \mathcal{P}_i = & N^{\text{Sig}} \times \frac{1}{2} [(1 - Q_i A^{\text{Sig}}) f \mathcal{P}_{\text{SCF},i}^{\text{Sig}} \\ & + (1 - Q_i A^{\text{Sig}})(1 - f) \mathcal{P}_i^{\text{Sig}}] \\ & + \sum_j N_j^{\text{Bkg}} \times \frac{1}{2} (1 - Q_i A_j^{\text{Bkg}}) \mathcal{P}_{j,i}^{\text{Bkg}}, \end{aligned}$$

where Q_i is the charge of the kaon in the event, $N^{\text{Sig}}(N_j^{\text{Bkg}})$ and $A^{\text{Sig}}(A_j^{\text{Bkg}})$ are the yield and asymmetry for signal and background component j , respectively, and $f = 35.5\%$ is the fraction of SCF signal events. The j individual background terms comprise continuum, $b \rightarrow c$ decays, K^{**} , and 13 exclusive charmless B decay modes. The PDF for each component, in turn, is the product of the PDFs for each of the fit input variables, $\mathcal{P} = \mathcal{P}_{m_{ES},\Delta E} \mathcal{P}_{ANN} \mathcal{P}_{m_{K\pi}}$. Due to correlations between ΔE and m_{ES} , the $\mathcal{P}_{m_{ES},\Delta E}$ for signal and all background from B decays are described by two-dimensional non-parametric PDFs [18] obtained from MC. For continuum background, the correlations in ΔE and m_{ES} are $\sim 1\%$, hence a separate PDF is used for each of them; m_{ES} is well described by an empirical phase-space threshold function [19] and ΔE is parameterized with a second degree polynomial. The parameters of the continuum PDFs are floated in the fit. ANN is described by a non-parametric PDF for continuum background and by a Crystal Ball function [20] for all other modes. For $\mathcal{P}_{m_{K\pi}}$, one-dimensional non-parametric PDFs obtained from MC are used to describe all modes except the signal mode itself, which is described by a Breit-Wigner line-shape combined with a first degree polynomial. The parameters for this PDF are held fixed to the MC values and varied within errors to estimate systematic uncertainties.

A number of cross checks confirm that the fit is unbiased. In 1000 separate MC experiments we generate the expected number of events for the various fit components before using the maximum likelihood fit to extract the yields and asymmetries. The distributions for each component are generated from the component's PDF, giving values for the fit variables m_{ES} , ΔE , ANN , and $m_{K\pi}$. The expected number of events is calculated from the branching fraction and efficiency for each individual

TABLE I: Breakdown of systematic uncertainties.

Absolute systematic uncertainties on yields	
Source	$\sigma_{\text{Syst.}}^{\text{Yield}}$ (Events)
Background normalization	± 14
PDF shapes	+ 2.1 - 4.0
SCF fraction	± 1.8
ΔE shift	± 2.2
Total	± 14
Relative systematic uncertainties on $\mathcal{B}(B^{\pm} \rightarrow K^{*\pm}\pi^0)$	
Source	$\sigma_{\text{Syst.}}^{\mathcal{B}}$ (%)
Efficiency estimation	± 7.3
B counting	± 1.1
Total	± 7.4
Systematic uncertainties on \mathcal{A}_{CP}	
Source	$\sigma_{\text{Syst.}}^{\mathcal{A}_{CP}}$
Background normalization	+0.018 -0.010
Detector asymmetry	± 0.003
Background asymmetry	+0.049 -0.041
Total	+0.054 -0.043

mode. The generated number of events for each fit component is determined by fluctuating the expected number according to a Poisson distribution. The test is repeated using samples with differing asymmetry values. We repeat these MC studies using fully simulated signal $B^{\pm} \rightarrow K^{*\pm}\pi^0$ events instead of generating the signal component from our PDFs. This verifies that the signal component is correctly modeled including correlations between the fit variables. Finally, omitting $m_{K\pi}$ as a fit variable has no significant influence on the signal yield, indicating that our treatment of K^{**} background is indeed effective.

Individual contributions to the systematic uncertainty are summarized in Table I. We calculate the uncertainty of the continuum background estimation directly from the fit to data. The backgrounds from B decays are determined from simulation and fixed according to their efficiencies and branching fractions. For those individual decay modes which have been measured we vary the number of events in the fit by their measured uncertainty. For all others we vary the amount included in the fit by $\pm 100\%$. For the $b \rightarrow c$ component we fix the rate based on the number calculated from MC samples and vary the amount based on the statistical uncertainty of this number (6%). The shifts in the fitted yields are calculated for each mode in turn and then added in quadrature to find the total systematic effect. The largest individual contribution comes from the K^{**} estimation.

To take into account the variation of the two-dimensional non-parametric PDFs used for ΔE and m_{ES} , we smoothen the MC-generated distributions from which the PDFs are derived. For $m_{K\pi}$ and ANN , the param-

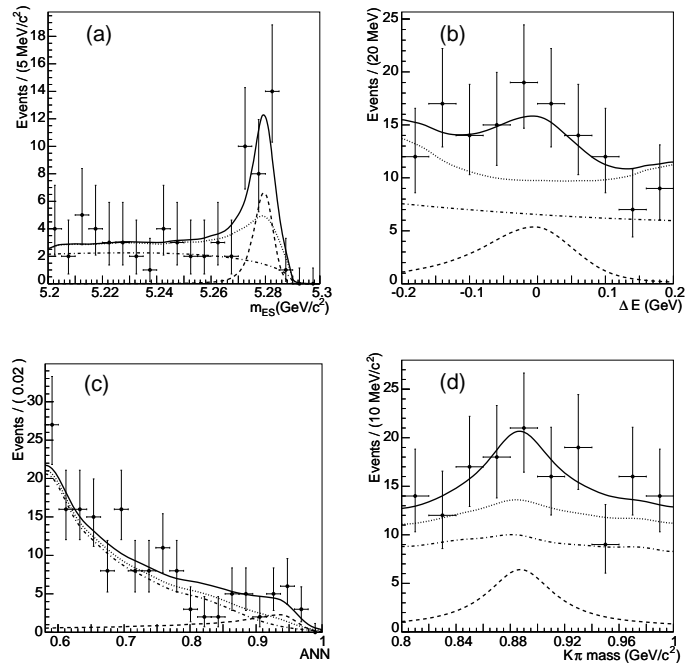


FIG. 1: Likelihood projection plots for the four fit variables, (a) m_{ES} , (b) ΔE , (c) ANN , and (d) $m_{K\pi}$. In each plot the solid line represents the total PDF, the dotted line represents the total background, the dotted-dashed line represents the continuum contribution, and the dashed line represents the signal component. The plots contain a subset of the events defined by a likelihood ratio of at least 0.1 (see text).

terizations determined from fits to MC events are varied by one standard deviation. The systematic uncertainties are determined using the altered PDFs and fitting to the final data sample. The overall shifts in the central value are taken as the size of the systematic uncertainty.

We vary the SCF fraction by a conservative estimate of its relative uncertainty ($\pm 10\%$) and assign the shift in the fitted number of signal events as the systematic uncertainty of the SCF fraction.

To account for differences in the neutral-particle reconstruction between data and MC simulation the signal PDF distribution in ΔE is offset by ± 5 MeV and the data refitted. The larger of the two shifts in the central value of the yield is 2.2 events, which is taken as the systematic uncertainty for this effect.

Corrections to the π^0 energy distribution, determined using various control samples, add a systematic uncertainty of 7.2%. A relative systematic uncertainty of 1% is assumed for the kaon identification. A relative systematic uncertainty of 0.8% on the efficiency for a single charged track is applied. Adding all the above contributions in quadrature gives a relative systematic uncertainty on \mathcal{B} of 7.3%. Another contribution of 1.1% comes from the uncertainty on the total number of B events.

The cross section for the interaction of kaons with protons and neutrons differs with charge. At low momenta

this can introduce a bias to the observed charge asymmetry. We estimate this bias by modelling the average loss of kaons from a sample based on the $K^{*\pm}\pi^0$ signal MC using the known detector material constants, and find $\mathcal{A}_{Kp} = -0.0031 \pm 0.0006$, which is negligible compared to the precision at which we measure \mathcal{A}_{CP} .

To calculate the effects of systematic shifts in the charge asymmetries of background modes, each mode is varied by its measured uncertainty. For contributions with no measurement, we assume zero asymmetry and assign an uncertainty of 20%, motivated by the largest charge asymmetry measured in any mode so far [9]. The individual shifts are then added in quadrature to find the total systematic uncertainty. The greatest individual contribution comes from the K^{**} estimate. In addition, the effect of altering the normalizations of the B backgrounds affects the fitted asymmetry. The size of the shift on the fitted \mathcal{A}_{CP} is taken as the size of the systematic uncertainty.

A total of 23,465 events were fitted, of which 11,960 had positively charged candidates. The central value of the signal yield from the maximum likelihood fit is 89 ± 26 events, over an expected background of 634 ± 40 events from other B decays. We obtain a branching fraction of $\mathcal{B}(B^\pm \rightarrow (K^{*\pm} \rightarrow K^\pm\pi^0)\pi^0) = [2.31 \pm 0.67 \pm 0.42] \times 10^{-6}$ and charge asymmetry of $\mathcal{A}_{CP}(B^\pm \rightarrow (K^{*\pm} \rightarrow K^\pm\pi^0)\pi^0) = 0.04 \pm 0.29 \pm 0.05$, where the first error is statistical and the second one systematic. Alternatively, we calculate the 90% confidence upper limit on the $B^\pm \rightarrow (K^{*\pm} \rightarrow K^\pm\pi^0)\pi^0$ branching fraction to be 3.9×10^{-6} . Compared against the null hypothesis, the statistical significance $\sqrt{-2\ln(\mathcal{L}_{Null}/\mathcal{L}_{Max})}$ of the yield amounts to 4.1 standard deviations. The fit was redone fixing the signal yield to the lowest yield allowed accounting for all possible combinations of systematic uncertainties. The significance of this result corresponds to 3.6 standard deviations.

The results of the fit are illustrated in Fig. 1. The plots are enhanced in signal by selecting only those events which exceed a threshold of 0.1 for the likelihood ratio $R = (N^{\text{Sig}}\mathcal{P}^{\text{Sig}})/(N^{\text{Sig}}\mathcal{P}^{\text{Sig}} + \sum_i N_i^{\text{Bkg}}\mathcal{P}_i^{\text{Bkg}})$, where N are the central values of the yields from the fit and \mathcal{P} are the PDFs with the projected variable integrated out. This threshold is optimized by maximizing the ratio $S = (N^{\text{Sig}}\epsilon^{\text{Sig}})/(\sqrt{N^{\text{Sig}}\epsilon^{\text{Sig}} + \sum_i N_i^{\text{Bkg}}\epsilon_i^{\text{Bkg}}})$ where ϵ are the efficiencies after the threshold is applied. The PDF components are then scaled by the appropriate ϵ .

In conclusion, we have measured the charge asymmetry and branching fraction for the decay $B^\pm \rightarrow (K^{*\pm} \rightarrow K^\pm\pi^0)\pi^0$ using a maximum likelihood fit. Assuming a secondary branching fraction of 1/3 for the $K^{*\pm} \rightarrow K^\pm\pi^0$ final state our result implies $\mathcal{B}(B^\pm \rightarrow K^{*\pm}\pi^0) = [6.9 \pm 2.0 \pm 1.3] \times 10^{-6}$, and a charge asymmetry of $\mathcal{A}_{CP} = 0.04 \pm 0.29 \pm 0.05$ where the first error is statistical and the second error systematic. The statistical significance of the branching fraction result including systematic uncertainties is calculated to be 3.6 standard deviations, showing evidence for this decay. The systematic error of the branching fraction and asymmetry is dominated by the contribution of K^{**} resonances.

We are grateful for the excellent luminosity and machine conditions provided by our PEP-II colleagues, and for the substantial dedicated effort from the computing organizations that support BABAR. The collaborating institutions wish to thank SLAC for its support and kind hospitality. This work is supported by DOE and NSF (USA), NSERC (Canada), IHEP (China), CEA and CNRS-IN2P3 (France), BMBF and DFG (Germany), INFN (Italy), FOM (The Netherlands), NFR (Norway), MIST (Russia), and PPARC (United Kingdom). Individuals have received support from CONACyT (Mexico), A. P. Sloan Foundation, Research Corporation, and Alexander von Humboldt Foundation.

-
- [1] N. Cabibbo, Phys. Rev. Lett. **10**, 531 (1963).
 [2] M. Kobayashi and T. Maskawa, Prog. Theor. Phys. **49**, 652 (1973).
 [3] M. Beneke and M. Neubert, Nucl. Phys. B **675**, 333 (2003).
 [4] C.-W. Chiang, M. Gronau, Z. Luo, J. Rosner, and D. Suprun, Phys. Rev. D **69**, 034001 (2004).
 [5] M. Ciuchini, E. Franco, G. Martinelli, and L. Silvestrini, Nucl. Phys. B **501**, 271 (1997).
 [6] M. Ciuchini, E. Franco, G. Martinelli, M. Pierini, and L. Silvestrini, Phys. Lett. B **515**, 33 (2001).
 [7] C. Isola, M. Ladisa, G. Nardulli, and P. Santorelli, Phys. Rev. D **68**, 114001 (2003).
 [8] D. Atwood and A. Soni, Phys. Rev. D **58**, 036005 (1998).
 [9] B. Aubert *et al.* (BABAR Collaboration), Phys. Rev. Lett. **93**, 131801 (2004).
 [10] Y. Chao *et al.* (BELLE Collaboration), Phys. Rev. Lett. **93**, 191802 (2004).
 [11] B. Aubert *et al.* (BABAR Collaboration), Phys. Rev. Lett. **94**, 181802 (2005).
 [12] A. Garmash *et al.* (BELLE Collaboration), Phys. Rev. D **65**, 092005 (2002).
 [13] B. Aubert *et al.* (BABAR Collaboration), Nucl. Instr. Methods Phys. Res., Sect. A **479**, 1 (2002).
 [14] B. Aubert *et al.* (BABAR Collaboration), Phys. Rev. D **69**, 071101 (2004).
 [15] A. Drescher *et al.* (ARGUS Collaboration), Nucl. Instr. Methods Phys. Res., Sect. A **237**, 464 (1985).
 [16] B. Aubert *et al.* (BABAR Collaboration), Phys. Rev. Lett. **89**, 201802 (2002).
 [17] S. Eidelman *et al.* (Particle Data Group), Phys. Lett. B **592**, 1 (2004).
 [18] K. Cranmer, Comput. Phys. Commun. **136**, 198 (2001).
 [19] H. Albrecht *et al.* (ARGUS Collaboration), Phys. Lett. B **241**, 278 (1990).
 [20] T. Skwarnicki (Crystal Ball Collaboration), Ph.D. thesis, Cracow Institute of Nuclear Physics (1986), DESY-F31-86-02.